

# Enhanced activity of the myocardial $\text{Na}^+/\text{H}^+$ exchanger contributes to left ventricular hypertrophy in the Goto–Kakizaki rat model of type 2 diabetes: critical role of Akt

A. Darmellah · D. Baetz · F. Prunier · S. Tamareille ·  
C. Rücker-Martin · D. Feuvray

Received: 23 August 2006 / Accepted: 7 January 2007 / Published online: 11 April 2007  
© Springer-Verlag 2007

## Abstract

**Aims/hypothesis** Diabetes mellitus is a strong risk factor for the development of heart failure, and left ventricular (LV) hypertrophy has been detected in a significant proportion of diabetic patients. Because several studies have suggested that the  $\text{Na}^+/\text{H}^+$  exchanger (NHE1) plays a part in the molecular mechanisms involved in cardiac hypertrophy, we investigated its activity and its role in LV myocytes from the Goto–Kakizaki (GK) rat model of type 2 diabetes.

**Materials and methods** Fluorometric measurements were used to assess sarcolemmal NHE1 activity in isolated myocytes. NHE1 levels and the possible molecular pathways driving and/or related to NHE1 activity were investigated in relation to the diabetic LV phenotype.

**Results** Enhanced NHE1 activity was associated with LV myocyte hypertrophy. This occurred in the absence of any change in NHE1 protein levels; however, activation of several molecular pathways related to NHE1 activity was demonstrated. Thus, phosphorylation of the extracellular signal-regulated protein kinase (Erk), of the protein kinase Akt (also known as protein kinase B) and of the  $\text{Ca}^{2+}/$

calmodulin-dependent kinase II was increased in GK LV myocytes. Intracellular  $\text{Ca}^{2+}$  levels were also increased. Chronic treatment (10–12 weeks) with the NHE1 inhibitor cariporide normalised NHE1 activity, decreased  $\text{Ca}_i^{2+}$  levels and reduced LV myocyte hypertrophy. Moreover, among the various activated pathways, cariporide treatment markedly reduced Akt activity only.

**Conclusions/interpretation** These findings indicate that activation of the Akt pathway represents a likely mechanism mediating the hypertrophic effect of increased NHE1 activity in the GK model of type 2 diabetes.

**Keywords** Akt/PKB kinase · Cardiac complications · GK rats · Left ventricular hypertrophy ·  $\text{Na}^+/\text{H}^+$  exchanger

## Abbreviations

$\beta$ -MHC	$\beta$ myosin heavy chain
CaMKII	calmodulin-dependent protein kinase II
cSNARF	carboxysemaphorhodafuor
ERK	extracellular signal-regulated protein kinase
GK	Goto–Kakizaki
LV	left ventricular
MAPK	mitogen-activated protein kinase
NHE	$\text{Na}^+/\text{H}^+$ exchanger
V:S	volume:surface area

## Introduction

Over recent years, the prevalence of diabetes mellitus, particularly type 2 diabetes, has increased significantly. Both clinical and experimental studies [1–4] have pointed to cardiomyopathy in humans producing abnormalities in ventricular function, independently from coronary artery

---

A. Darmellah · D. Baetz · S. Tamareille · C. Rücker-Martin ·  
D. Feuvray (✉)  
Marie Lannelongue Hospital,  
UMR CNRS 8078—University of Paris South XI,  
133 Avenue de la Résistance,  
92350 Le Plessis Robinson, France  
e-mail: danielle.feuvray@u-psud.fr

F. Prunier  
IFR 02, Xavier Bichat Medical School,  
Paris, France

F. Prunier  
Department of Cardiology, University Hospital,  
Angers, France

disease or hypertension. However, few experimental studies on cardiac function have been conducted using animal models of type 2 diabetes [5–7]. The Goto–Kakizaki (GK) rat is a genetic model of type 2 diabetes produced by selective inbreeding of mildly glucose-intolerant Wistar rats [8]. Alterations in glucose and insulin metabolism in this model are caused by at least six independent genetic loci [9]. GK rats have a stable, inheritable form of type 2 diabetes characterised by mild hyperglycaemia and hyperinsulinaemia, and no obesity, hypertension or marked hyperlipidaemia [8, 9]. The GK rat thus offers a convenient model for the study of type 2 diabetes, without the confounding effects of obesity or hypertension per se. A recent report of possible cardiac complications in this potentially relevant type 2 diabetes-like GK rat has suggested that cardiac hypertrophy is present in this model [7].

The cardiac sarcolemmal  $\text{Na}^+/\text{H}^+$  exchanger (NHE1) has recently gained considerable interest in the context of myocardial damage [10]. In previous studies, we have shown that the streptozotocin-induced model of type 1 diabetes in rats is associated with a decrease in NHE1 activity [11–13]. With regard to myocardial ischaemia/reperfusion injury, several studies have already shown that inhibition of this exchanger results in significant protection of the reperfused ischaemic myocardium [11, 14]. In addition to its role in ischaemia and reperfusion, the exchanger is likely of importance in other cardiac disease states. Thus, several recent studies have suggested that activation of the NHE1 plays a role in the molecular mechanisms responsible for cardiac hypertrophy [15–17]. However, to date, no study has examined myocardial NHE1 activity in type 2 diabetes.

Because diabetes mellitus is a strong risk factor for the development of heart failure, and given that left ventricular (LV) hypertrophy has been detected in a significant proportion of type 2 diabetic patients [2, 3], we decided to examine the activity and role of NHE1 in LV myocytes from GK rats. In addition, we evaluated whether treatment with the selective NHE1 inhibitor cariporide [18] influences the diabetic LV phenotype when applied for a few weeks after weaning. We also investigated the possible molecular pathways driving and/or related to NHE1 activity in relation to the diabetic LV phenotype of GK rats.

## Materials and methods

**Experimental animals** Animal care and procedures were in accordance with the guidelines formulated by the European Convention for the Protection of Vertebrate Animals used for Experimental Purposes, and institutional guidelines (no. 86/609/CEE 24 November 1986). Male diabetic GK rats

were obtained from the Paris colony at the University of Paris VII [8, 9]. Age-matched Wistar rats were used as control animals. The animals were fed either a standard diet (untreated Wistar and GK rats) or a diet containing 6 g/kg of the selective NHE1 inhibitor cariporide (Aventis Pharma, Frankfurt, Germany) beginning at 4 weeks of age for 10–12 weeks. This resulted in plasma levels of cariporide of  $\sim 2.3 \mu\text{mol/l}$  [17, 18]. Heart rate and blood pressure were monitored using a telemetric pressor transducer (DataQuest IV software; Data Sciences, Saint Paul, MN, USA). Glucose levels were determined by enzymatic colorimetry, and insulin was analysed by double-antibody radioimmunoassay (rat insulin ELISA; Mercodia, Uppsala, Sweden) in plasma samples collected at the time of heart excision (post-absorptive state). After quickly removing and weighing the heart, tibia length was also determined.

**Echocardiography** Echocardiography was performed with a Toshiba Powervision 6000 device (model no. SSA 370A; Toshiba, Puteaux, France), equipped with an 8 to 14-MHz linear transducer, under isoflurane anaesthesia (1.0–1.5% in oxygen) and spontaneous ventilation. LV global systolic and diastolic functions were assessed as described previously [19].

**Immunolabelling and confocal microscopy** Hearts were rinsed in phosphate-buffered saline, immediately frozen in liquid nitrogen, and then stored at  $-80^\circ\text{C}$ . Frozen sections (10  $\mu\text{m}$ ) were fixed in methanol at  $-20^\circ\text{C}$  for 10 min, incubated with the monoclonal antibody directed against the slow myosin heavy chain (anti- $\beta$ -MHC) (1:20 dilution; Novocastra, Newcastle, UK) and then with the anti-mouse IgG coupled to Alexa Fluor 488 (green, 1:100 dilution; Invitrogen, Paisley, UK) [20]. Sections were analysed by confocal scanning laser microscopy (Leica Microsystems, Mannheim, Germany) at a magnification of  $\times 400$  by measurement of mean fluorescence intensity (FI, using a range of 0–255 AU) [20].

**Individual myocyte measurements** To assess myocyte dimensions, sarcolemmal NHE1 [13] or cellular kinase [21] activity, individual myocytes were isolated from the LV wall of perfused hearts using a combination of enzymatic and mechanical dispersion [13, 21].

Cell dimensions were measured on a calibrated monitor in conjunction with the  $\times 40$  objective lens of a microscope, using ImageJ software (<http://rsb.info.nih.gov/ij/>, last accessed in January 2007). The volumes of myocytes were calculated from the length and width of each cell, using the following formula:  $\text{volume} = \text{width} \times \text{length} \times 0.00759 \text{ pl}/\mu\text{m}^2$  [22]. To obtain an estimate of cell surface area, membrane capacitance was calculated by measuring the resistance in series and the time constant of the experimental decay of

the capacitive transient elicited by a 10 mV depolarising pulse, as described previously [23].

A microepifluorescence technique was used to record intracellular pH ( $\text{pH}_i$ ) in single myocytes loaded with 5  $\mu\text{mol/l}$  cSNARF-1, and the rate of acid efflux ( $J_H = \beta_i \times \text{dpH}_i/\text{dt}$ , where  $\beta_i$  is intracellular buffering power), calculated at  $\text{pH}_i$  intervals of 0.05 during recovery from intracellular acidosis, was used as an indicator of sarcolemmal NHE1 activity [13]. Since NHE1 is nearly quiescent at a resting  $\text{pH}_i$  of  $\geq 7.1$ , addition and then removal of  $\text{NH}_4\text{Cl}$  (10 mmol/l) was used to induce intracellular acidification to activate NHE1 in bicarbonate-free HEPES-buffered Tyrode's solution [13]. All solutions had a pH of 7.4 at 37°C. When used, the  $\text{Ca}^{2+}$ /calmodulin-dependent protein kinase II (CaMKII) inhibitor KN-62 (Sigma, St Louis, MO, USA) was present from 8 min before the  $\text{NH}_4\text{Cl}$  pre-pulse, and the  $\text{Ca}^{2+}$ -dependent protein kinase C (PKC) inhibitor Gö6976 or the non-specific PKC inhibitor GF109203X or the Akt (also known as protein kinase B) inhibitor API-2 (Merck Biosciences, Nottingham, UK) was present from 20 min before the  $\text{NH}_4\text{Cl}$  pre-pulse (all inhibitors dissolved in dimethyl sulfoxide, final concentration  $<0.1\%$ ). Intracellular  $\text{Ca}^{2+}$  ( $\text{Ca}_i^{2+}$ ) was monitored using the Indo-1 technique, as previously described [24]. All experiments were performed at  $36 \pm 1^\circ\text{C}$ .

Whole-cell lysates (20–40  $\mu\text{g}$  protein) [21] were resolved by SDS-PAGE and immunoblotted with specific antibodies to phosphorylated extracellular signal-regulated protein kinases 1 and 2 (phospho-ERK1/2), p38 MAPK, phospho-p38 MAPK, Akt, phospho-Akt (Cell Signaling Technology, Beverly, MA, USA), ERK2, JNK, phospho-JNK, CaMKII and phospho-CaMKII (Santa Cruz Biotechnology, CA, USA) and appropriate secondary antibodies (goat anti-rabbit and goat anti-mouse horseradish peroxidase conjugates; Amersham Biosciences, Freiburg, Germany). To quantify the extent of phosphorylation of each kinase, the phosphorylated band density was expressed relative to the intensity of the total protein band.

**Determination of NHE1 levels** Myocardial levels of NHE1 were determined at protein level by immunoblot analysis. We used unfractionated tissue homogenates as described previously [25]. LV tissue samples were rapidly thawed, weighed and homogenised for 3–4 min in lysis buffer (5% sorbitol, 25 mmol/l histidine pH 7.4, 50 mmol/l  $\text{Na}_2\text{EDTA}$ , 50 mmol/l KCl, protease inhibitor cocktail). 0.5% SDS and 0.1% 2-mercaptoethanol were added to 25  $\mu\text{l}$  of sample containing 100  $\mu\text{g}$  of protein. The samples were boiled for 5 min, and then 55  $\mu\text{l}$  of lysis buffer and 5  $\mu\text{l}$  of polyoxyethylene-8-lauryl ether (Sigma) were added to them. After incubation at 37°C for 15 h, 50  $\mu\text{l}$  of 3 $\times$  SDS sample buffer was added, and then the samples were boiled

for 10 min. Samples (100  $\mu\text{g}$  protein) were subjected to electrophoresis through a 7.5% SDS-polyacrylamide gel, and the separated proteins were transferred onto polyvinylidene difluoride membranes. Immunoblot analysis was performed using a mouse monoclonal antibody directed against NHE1 (Chemicon, Temecula, CA, USA) in conjunction with anti-mouse secondary antibody and an enhanced chemiluminescence detection system (Amersham Biosciences).

**Statistical analysis** Data are presented as means $\pm$ SEM. Statistical analysis of the results was performed using either the Student's *t* test or ANOVA followed by Tukey post-hoc test to identify differences between groups. Significance was set at  $p < 0.05$ .

## Results

GK rats had mild hyperglycaemia; however, basal plasma insulin levels were not significantly different from those in Wistar rats. The systolic BP was similar for the two groups (Table 1). Average body weight was slightly lower in GK rats than in Wistar rats of the same age. These observations are in agreement with previous studies [7].

**Expression of the diabetic cardiomyopathy phenotype** On echocardiography (Table 1), LV wall thickness was increased in GK rats compared with that in Wistar rats; LV ejection fraction was reduced, whereas isovolumic relaxation time was increased. This is in line with reports showing abnormalities in cardiac contractile performance and sarcoplasmic reticulum function in other models of type 2 diabetes [26, 27]. Biventricular weight normalised by body weight was significantly higher in GK rats, suggesting cardiac hypertrophy (Fig. 1a). However, since there were changes in body weight in GK rats, biventricular weight was more accurately normalised by tibial length (Fig. 1b). When normalised by tibial length or body weight, relative to hearts of Wistar rats, GK rat hearts showed 22 and 20% hypertrophy, respectively. To evaluate the hypertrophic response at the LV myocyte level, whole-cell membrane capacitance was used as a measure of cell surface area, and  $\beta$ -MHC immunolabelling as a marker of cell hypertrophy [28]. Figure 1c shows that the membrane capacitance of LV myocytes from GK rats was significantly increased compared with that of LV myocytes from Wistar rats ( $p < 0.001$ ). Moreover, as illustrated in Fig. 2, there was a much larger amount of  $\beta$ -MHC detected in GK LV myocytes (47% of area sections) than in Wistar LV myocytes (~2%). Figures 1 and 2 also show that cariporide treatment significantly attenuated the expression of the hypertrophic phenotype in diabetic GK rat hearts, since it

**Table 1** Characteristics of Wistar and GK rats

	Wistar		GK	
	<i>n</i>	Value	<i>n</i>	Value
Body weight (g)	23	376±11	23	330±4*
Plasma glucose (mmol/l)	30	9.4±0.3	30	14.3±0.2*
Plasma insulin (pmol/l)	30	150±21	30	176±23
Systolic blood pressure (mmHg)	10	131±2	10	134±2
Echocardiography				
Heart rate (beats per min)	8	322±8	10	328±9
AW/BW (mm/kg)	8	3.5±0.1	10	4.8±0.2*
PW/BW (mm/kg)	8	3.5±0.2	10	4.8±0.2*
EF (%)	8	80±2	10	73±1*
IVRT (ms)	8	25.3±0.8	10	28.3±0.6*

Values are means ± SEM.

*BW* body weight, *AW* anterior end-diastolic wall thickness, *PW* posterior end-diastolic wall thickness, *EF* ejection fraction, *IVRT* isovolumic relaxation time. \* $p < 0.05$  for difference from Wistar rats

reduced the normalised biventricular weight, as well as the increase in LV myocyte membrane capacitance and the percentage area of LV myocyte  $\beta$ -MHC-specific labelling.

**Enhanced activity of NHE1 in LV myocytes of diabetic GK rats** We next examined NHE1 activity in LV myocytes isolated from GK rats. Steady-state  $\text{pH}_i$  values were  $7.25 \pm 0.03$  and  $7.32 \pm 0.02$  in GK and Wistar myocytes, respectively (both  $n=20$ ,  $p=0.111$ ). Representative recordings of  $\text{pH}_i$  recovery from an intracellular acid load are shown in Fig. 3a. It is clear that  $\text{pH}_i$  recovery from acidification was faster in GK LV myocytes than in Wistar LV myocytes, suggesting increased NHE1 activity. However, as illustrated in Fig. 3b,  $\text{pH}_i$  recovery in diabetic LV myocytes isolated from cariporide-treated GK rats was not different from that recorded in Wistar LV myocytes. Quantitative analysis of  $\text{pH}_i$  data, expressed as acid efflux carried by NHE1 (Fig. 3c), revealed that type 2 diabetes in GK LV myocytes is associated with significantly greater NHE1 activity, especially at  $\text{pH}_i$  values of 6.9 and 6.8 (greater than 100% increase). Data in Fig. 3c also indicate that cariporide

treatment prevented the diabetes-associated increase in NHE1 activity but did not effect NHE1 activity in Wistar LV myocytes. It should be noted that intrinsic buffering power ( $\beta_i$ ), estimated over this  $\text{pH}_i$  range, was similar in the two populations of myocytes (data not shown), and was not affected by cariporide treatment. Since it is only appropriate to compare such  $J_H$  values between cells with identical volume:surface area (V:S) ratios [22], we estimated the V:S ratios in the two groups of LV myocytes, both with and without cariporide treatment. The average V:S values (Fig. 3d) were not significantly different between the myocyte groups. These data therefore indicate enhanced NHE1 activity in LV myocytes of GK rat hearts, and that this enhanced NHE1 activity can be prevented by cariporide treatment.

**Basal  $\text{Ca}_i^{2+}$  levels in LV myocytes of GK rats** We postulated that enhanced NHE1 activity in GK LV myocytes may be associated with an increase in  $\text{Na}_i^+$ , which in turn causes an increase in  $\text{Ca}_i^{2+}$  mediated by the reverse mode of  $\text{Na}^+ - \text{Ca}^{2+}$  exchange [29, 30]. To test this hypothesis, basal  $\text{Ca}_i^{2+}$  levels were compared in LV myocytes obtained from GK and Wistar rats (Fig. 4a). GK myocytes had markedly increased  $\text{Ca}_i^{2+}$  levels (Indo-1 ratio:  $1.25 \pm 0.02$  vs  $0.97 \pm 0.02$ ,  $p < 0.001$ ). Cariporide treatment noticeably decreased  $\text{Ca}_i^{2+}$  levels in GK myocytes ( $1.02 \pm 0.02$ ) such that they were not significantly different from those in Wistar myocytes.

**Mechanisms for increased NHE1 activity in LV myocytes of GK rats** To investigate whether NHE1 protein levels could be influenced by type 2 diabetes we performed an immunoblot analysis of a random selection of LV myocardium from GK and Wistar rats, both cariporide-treated and untreated. The results revealed that NHE1 protein was present in similar abundance in all samples (Fig. 3e).

Although intracellular acidification is the major stimulus for NHE1 activation, molecular regulation occurs, at a given  $\text{pH}_i$ , through various proteins, some of which are  $\text{Ca}_i^{2+}$ -dependent. In a previous study we showed that changes in  $\text{Ca}_i^{2+}$  may play an important role in regulating NHE1 in

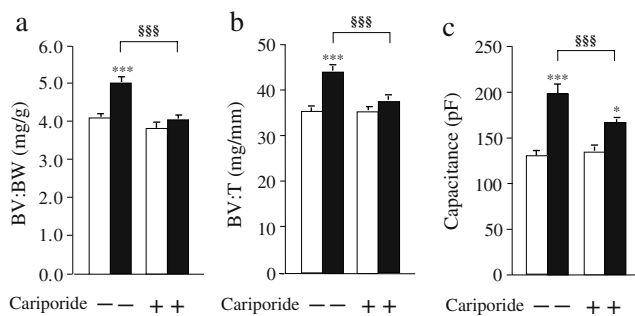


**Fig. 1** Diabetic hypertrophic phenotype expressed as ratios of biventricular weight:body weight (a) and biventricular weight:tibial length (b), and as LV myocyte membrane capacitance (c) in Wistar (open columns) and GK (filled columns) rats. The influence of cariporide treatment is shown for all measurements. Data shown are the means ± SEM of 22–28 animals per group (a, b) and of 25–30 LV myocytes from six to ten separate hearts per group (c). \* $p < 0.05$  vs treated or untreated Wistar rats, \*\*\* $p < 0.001$  vs Wistar rats, §§§ $p < 0.001$ . *BV* biventricular weight; *BW* body weight, *T* tibial length

cardiac myocytes [13]. Other work on fibroblasts has shown a role for protein kinase C $\alpha$  in growth factor-induced activation of NHE1 [31]. The results of pharmacological inhibition of CaMKII and protein kinase C on

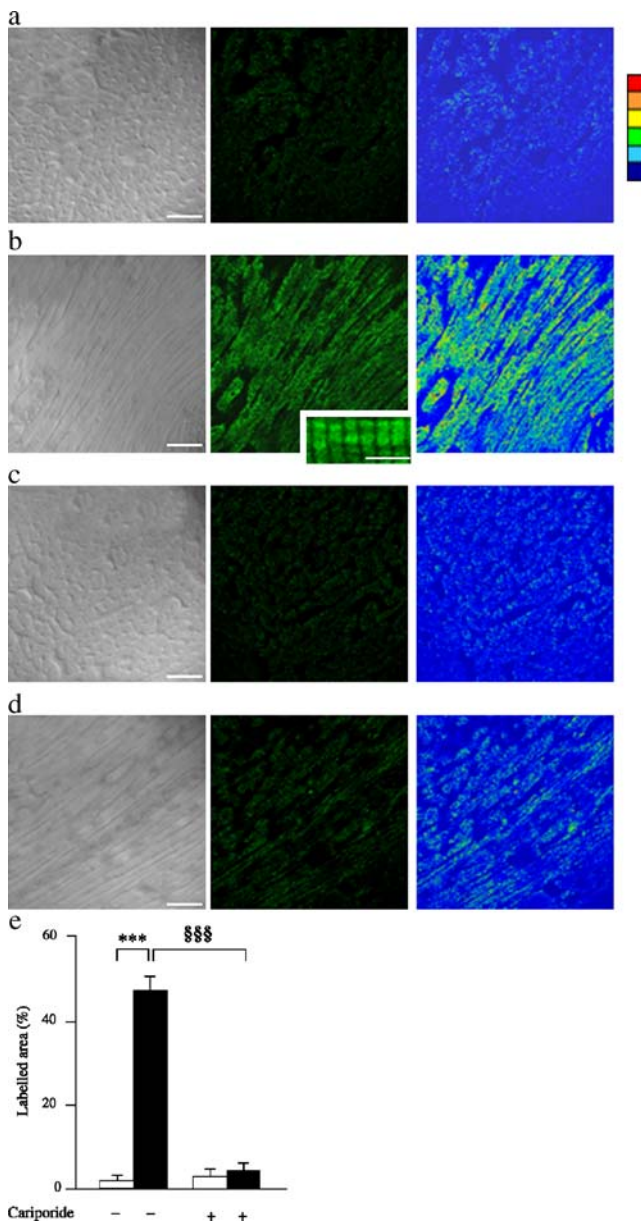


**Fig. 2** Confocal microscopy images of LV sections of untreated (a) and cariporide-treated (c) Wistar rats, and untreated (b) and cariporide-treated (d) GK rats. The *left-hand column* shows differential interference contrast views; the *middle column* shows  $\beta$ -MHC immunostaining (coded green), and the *right-hand column* shows pseudo-colour intensity maps (intensity scale shown to the upper right of the figure). The inset in GK  $\beta$ -MHC immunostaining (b, *centre panel*) is at higher magnification, illustrating the regular pattern of sarcomeric band A labelling by the antibody. For each group, 25–30 test areas were analysed in three to four hearts per group. *Horizontal bars* in panels=50  $\mu$ m; *horizontal bar* in the inset=10  $\mu$ m. **e** Bar graph showing the mean $\pm$ SEM percentage of positive cell labelling area in treated and untreated GK rats (*filled columns*) and Wistar rats (*open columns*). \*\*\* $p < 0.001$ , §§§ $p < 0.001$

NHE1 activity in GK and Wistar LV myocytes are shown in Fig. 4b. When the CaMKII inhibitor KN62 (2  $\mu$ mol/l [13]) was applied to Wistar LV myocytes, this slowed  $\text{pH}_i$  recovery following an acid load (data not shown) and there was an associated decrease in acid efflux ( $\sim 34\%$  decrease in  $J_{\text{H6.85}}$ ), as previously described [13], whereas similar application of this inhibitor resulted in a more marked effect in GK LV myocytes ( $\sim 56\%$  decrease). Inhibition of  $\text{Ca}^{2+}$ -dependent protein kinase C by Gö6976 (1  $\mu$ mol/l [32]) similarly inhibited acid efflux by NHE1 in GK LV myocytes; however, the same concentration of Gö6976 had no effect when applied to Wistar LV myocytes. Likewise, the non-specific protein kinase C inhibitor GF109203X (1  $\mu$ mol/l), which also significantly reduced  $J_{\text{H6.85}}$  in GK LV myocytes, had no effect on NHE1 activity in Wistar LV myocytes. Notably, none of these inhibitors had any additional effect on the reduced NHE1 activity (i.e.  $J_{\text{H6.85}}$ ) observed after cariporide treatment in GK LV myocytes.

A family of mitogen-activated protein kinases (MAPKs) that includes ERK 1/2, p38 MAPK and JNK has been shown to respond to a variety of cellular stresses, including changes in  $\text{pH}_i$  [21, 33, 34]. We therefore measured the levels and phosphorylation of these proteins, as well as those of the cell growth and survival kinase Akt [35, 36]. Figure 5a shows that basal ERK phosphorylation, and therefore activation, was similar in LV myocytes of untreated or treated GK and Wistar rats, and that ERK phosphorylation after induction of intracellular acidification was increased in both Wistar and GK LV myocytes. The increase in Wistar myocytes was relatively modest (47%) in agreement with our previous report [21], whereas it was more marked in GK LV myocytes, being nearly twofold higher than that in Wistar myocytes. Figure 5a also shows that the marked increase in ERK phosphorylation upon acidification in GK LV myocytes was not abolished by cariporide treatment, although there was a trend towards a lesser increase in ERK activity. Basal p38 and JNK phosphorylation were the same in both Wistar and GK LV myocytes and, in contrast to phospho-ERK data, remained unchanged after acidification in the two groups of myocytes (Fig. 5b and c). Because we found an effect of CaMKII inhibition on NHE1 activity, a change in phospho-CaMKII activity might be expected. As shown in Fig. 5d, basal levels of phospho-CaMKII were increased by  $\sim 36\%$  in GK myocytes relative to those in Wistar myocytes ( $p = 0.052$ ). Acidification further increased phospho-CaMKII levels, by  $\sim 50\%$  in GK myocytes, but by only  $\sim 35\%$  in Wistar myocytes. Notably, cariporide treatment of GK rats did not significantly ( $p = 0.082$ ) reverse the change in phospho-CaMKII activity. Levels of phospho-Akt (Fig. 6a), which were, on average, similar in the different groups of myocytes under basal conditions, were markedly increased by acidification in GK LV myocytes (by  $\sim 80\%$ ). A

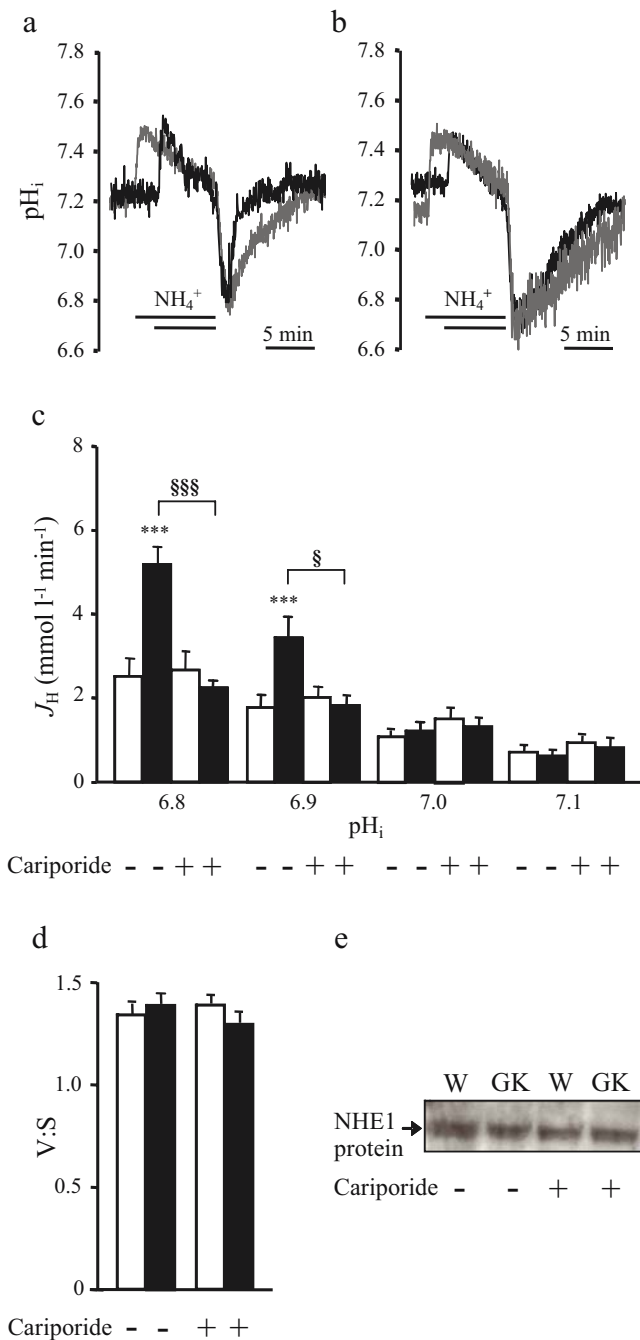


**Fig. 3** Activity of NHE1 in LV diabetic myocytes and the influence of cariporide treatment. Representative recordings of  $pH_i$  recovery from an intracellular acid load in myocytes isolated from untreated (a) and treated (b) Wistar (grey trace) and GK rat (black trace) hearts. **c** Bar graph of acid efflux ( $J_H$ ) by NHE1 in myocytes of untreated and treated Wistar (open columns) and GK (filled columns) rat hearts.  $J_H$  was calculated at four successive  $pH_i$  values (6.8, 6.9, 7.0 and 7.1) during recovery. Data are expressed as the means  $\pm$  SEM of six to seven cells from five to six separate hearts in each group. **d** Bar graph of V:S ratios of LV myocytes from untreated and treated Wistar (open columns) and GK (filled columns) rat hearts (70–80 cells from six to seven separate hearts per group). **e** Autoradiogram illustrating protein levels of NHE1 in LV samples from untreated and treated Wistar and GK rat hearts. Six to eight samples from three separate hearts in each group were examined. \*\*\* $p$ <0.001 vs Wistar rats, § $p$ <0.05, §§§ $p$ <0.001

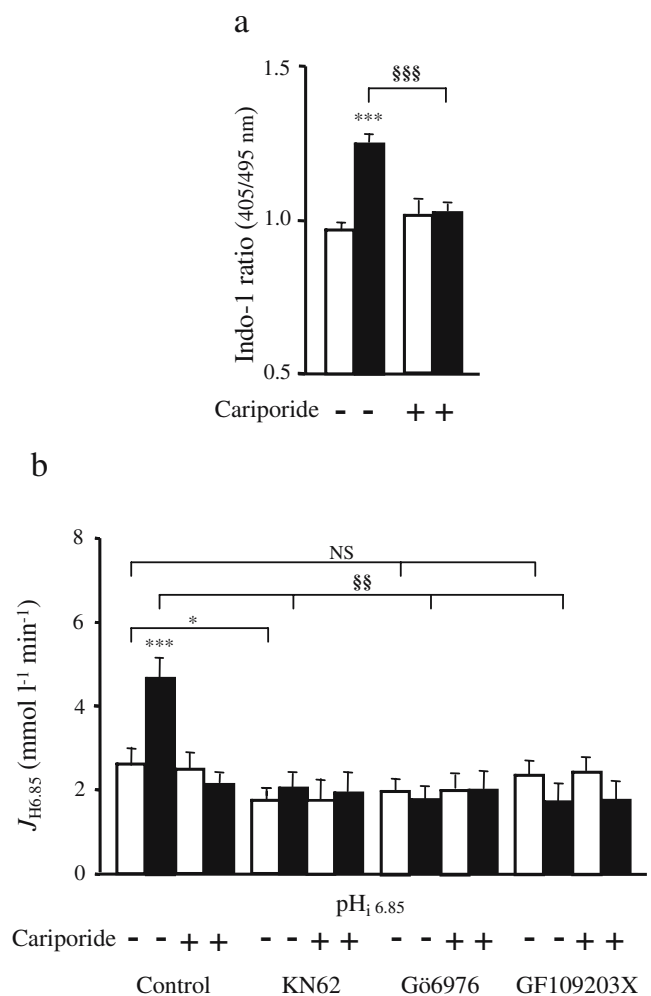


**Fig. 4** a  $Ca^{2+}_i$  levels expressed as Indo-1 fluorescence ratios in LV myocytes of untreated and treated GK (filled columns) and Wistar (open columns) rats. Data shown are the means  $\pm$  SEM of 18–25 myocytes from three to five separate hearts per group. **b** Bar graph of the effects of inhibition of CaMKII (KN62),  $Ca^{2+}$ -dependent protein kinase C (Gö6976) and non-specific protein kinase C (GF109203X) on NHE1 activity (acid efflux estimated at  $pH_i$  6.85) in LV myocytes from each group of rats. Data are expressed as the means  $\pm$  SEM of five to seven cells from three separate treated and five separate untreated GK (filled columns) and Wistar (open columns) rats. \* $p$ <0.05, \*\*\* $p$ <0.001 vs Wistar rats, §§ $p$ <0.01, §§§ $p$ <0.001

tendency for an increase in phospho-Akt was also noted in Wistar myocytes; however, this was not significant. Furthermore, it should be noted that phospho-Akt stimulation in acidified GK myocytes was totally prevented by cariporide treatment. Taken together, these data indicate that, although several pathways (ERK, CaMKII and Akt) were activated in GK LV myocytes, cariporide treatment was only efficient at markedly reducing the increase in Akt phosphorylation. To further clarify the role of the Akt pathway linking NHE1 activity to hypertrophy, we examined NHE1 activity in the presence of three different concentrations (1, 10 and 30  $\mu$ mol/l) of the

Akt inhibitor API-2 [37] (Fig. 6b and c). Clearly, none of these inhibitor concentrations had any effect on the rate of acid efflux, thus indicating that Akt is clearly downstream of NHE1.

## Discussion

The results of the present study demonstrate an increase in NHE1 activity in cardiac LV myocytes of the GK rat model of type 2 diabetes. This is accompanied by a phenotype of hypertrophy that can be prevented by chronic treatment with the NHE1 inhibitor cariporide. We also found that activation of the Akt pathway likely underlies the hypertrophic effect of increased NHE1 activity.

There are several possible explanations for the increased basal  $Ca_i^{2+}$  levels observed in GK myocytes. They could be related either to decreased sarcoplasmic reticulum  $Ca^{2+}$  uptake and/or to increased  $Ca^{2+}$  leakage, as shown in other models of type 2 diabetes [6, 26, 27]. They may also be the consequence of enhanced NHE1 activity [30]. Since cariporide treatment prevented any such increase, the latter explanation would appear the most probable. Increased  $Ca_i^{2+}$  levels themselves contribute to the activation of NHE1 by releasing a negative constraint in a particular subdomain of the NHE1 cytosolic region [38]. Previous work [13] has suggested that  $Ca_i^{2+}$  plays a role in the diabetes-related alterations of the exchanger in cardiac myocytes. But the effects of streptozotocin-induced diabetes in this study contradict those in the present work, since Le Prigent et al. reported that there was a decrease in NHE1 activity vs an increase in GK LV myocytes, and that this decrease in NHE1 activity was associated with a decrease in  $Ca_i^{2+}$  [24], whereas we found that increased NHE1 activity was associated with an increase in  $Ca_i^{2+}$ . NHE1 activity may be affected simply as a consequence of changes in  $Ca_i^{2+}$ , as mentioned above, and/or because of other alterations related to diabetes. It is of note that cariporide treatment of GK rats did not reverse the increased phospho-CaMKII, probably because the phosphorylation state of CaMKII reflects its  $Ca^{2+}$ -independent activity [39]. Some studies have suggested that the MAPK pathway may also play a role [33, 34]. We found there to be an increase in ERK phosphorylation following acidification in Wistar myocytes, in agreement with our previous observation [21], and a further increase in GK myocytes with greater sarcolemmal NHE1 activity. On the other hand, p38 and JNK phosphorylation status was unchanged following acidification in LV myocytes from both Wistar and GK rats. Another study [33] has also shown that stimulation of NHE1 activity with acidification requires activation of the ERK pathway but not the p38 pathway of the MAPK cascade in cardiomyocytes. Several recent

studies have suggested the existence of cross-talk between  $Ca_i^{2+}$  signalling and the MAPK pathway in multiple cell systems [32, 40]. Since  $Ca_i^{2+}$  was increased in GK LV myocytes, and specific inhibition of CaMKII and of  $Ca^{2+}$ -dependent protein kinase C reduced acid efflux carried by NHE1 (Fig. 4), such interplay may well be involved in increasing ERK activity. In a few preliminary experiments, we observed (data not shown) that  $Ca^{2+}$ -dependent protein kinase C inhibition with Gö6976 did indeed reduce the increase in ERK phosphorylation following acidification in GK, but not in Wistar myocytes, this effect being concentration dependent (decrease by ~50% at 10 nmol/l and by ~78% at 1  $\mu$ mol/l), whereas ERK phosphorylation did not seem to be affected by CaMKII inhibition with KN62 at 1  $\mu$ mol/l. Clearly, further work will be required to

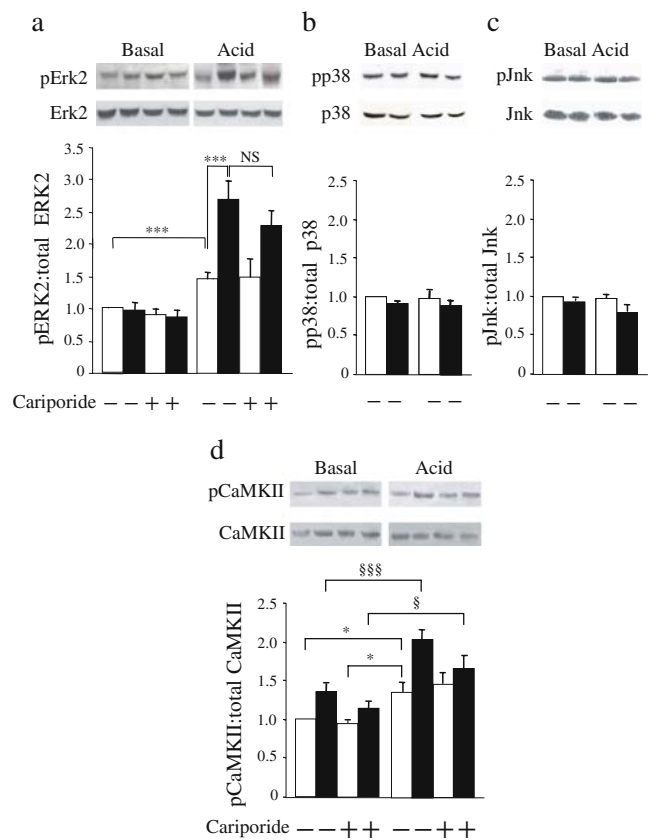


**Fig. 5** Activity of protein kinases under basal conditions and 1 min after acidification (acid) in LV myocytes of untreated and cariporide-treated Wistar and GK rats. Autoradiograms show representative western blots. For each of the kinases, whole-cell lysates were probed for the active form (phosphorylated) with anti-phosphospecific antibody (*upper bands*). The blots were stripped and reprobbed for anti-total antibody (*lower bands*). The bar graphs show the ratio of phosphorylated protein to total protein for each of the kinases in the GK (*filled columns*) and Wistar (*open columns*) rats. A value of 1 AU was assigned to the basal ratio for the Wistar rats. Data are from four to six experiments with cells from four Wistar and four GK hearts for each condition. \*  $p < 0.05$ , \*\*\*  $p < 0.001$

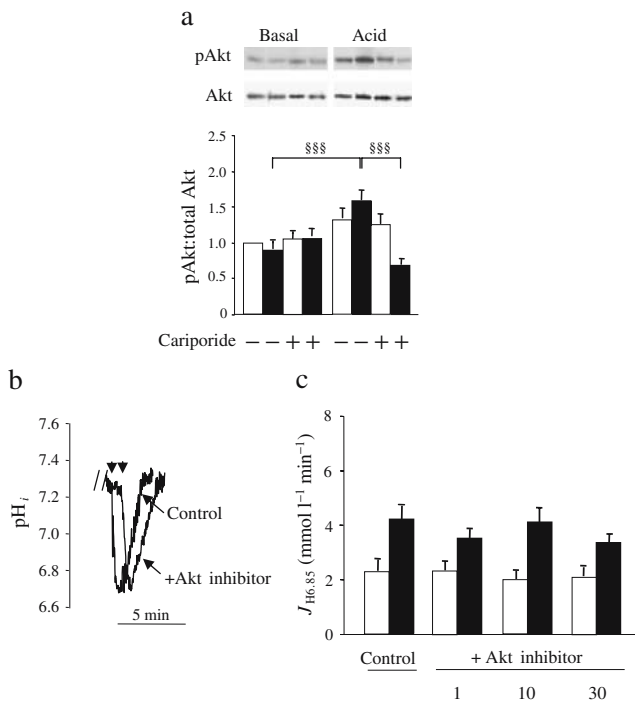


**Fig. 6** Akt activity under basal conditions and 1 min after acidification (acid) in LV myocytes of untreated and cariporide-treated Wistar and GK rats. **a** Autoradiograms show representative western blots. Whole-cell lysates were probed for the active form (phosphorylated) with anti-phosphospecific antibody (upper bands). The blots were stripped and reprobed for anti-total antibody (lower bands). The bar graphs show the ratio of phosphorylated/total kinase in the GK (filled columns) and Wistar (open columns) rats. A value of 1 AU was assigned to the basal ratio for the Wistar rats. Data are from four to six experiments with cells from four Wistar and four GK hearts for each condition.  $^{***}p < 0.001$ . **b**, **c** Activity of NHE1 in LV diabetic myocytes and the influence of Akt inhibition. **b** Representative recordings of  $pH_i$  recovery from an intracellular acid load in myocytes isolated from untreated diabetic GK rat hearts in the absence or presence of 10  $\mu\text{mol/l}$  of the Akt inhibitor API-2. The plots of the  $pH_i$  recovery in the two groups following acidification are superimposed to ease the comparison. Arrow heads indicate  $\text{NH}_4\text{Cl}$  removal. **c** Acid efflux ( $J_{\text{H6.85}}$ ) by NHE1 at  $pH_i$  6.85 in myocytes of untreated Wistar (open columns) and GK (filled columns) rat hearts in the absence or presence of Akt inhibitor at the micromolar concentrations. Data shown are the means  $\pm$  SEM of six to seven cells from five to six separate hearts in each group

clarify this point. Alternatively, it has been shown that ERK is regulated by an  $\text{Na}^+/\text{H}^+$  exchanger in rat aortic vascular smooth muscle cells [41]. Both the decrease in NHE1 activity and the decrease in  $\text{Ca}_i^{2+}$  after cariporide treatment would therefore seem to contribute to reducing ERK phosphorylation. However, under our experimental conditions, it was not normalised by cariporide treatment, which significantly attenuated the expression of the hypertrophic phenotype in GK LV myocytes.

An important and novel observation in this study is that intracellular acidification in cardiac ventricular myocytes, especially in GK LV myocytes, stimulated Akt phosphor-

ylation, and that this effect was totally prevented by NHE1 inhibition. A recent work using two different cell lines—a human renal epithelial cell line and LLC-PK1 cells [36]—has highlighted a major role for NHE1 in the regulation of Akt. We show here that this applies particularly to LV myocytes of type 2 diabetic GK rats. Wu et al. [36] demonstrated that activated NHE1 functions as a scaffold for recruitment of a signalplex that includes ezrin/radixin/moesin linkers, phosphoinositide 3-kinase and, ultimately, Akt. Akt then phosphorylates multiple substrates, thereby regulating the apoptotic response [36] as well as cell hypertrophy [35]. Several studies have indicated that chronic inhibition of NHE1 favourably interferes with the development of cardiac hypertrophy [16, 17, 42, 43]. Recently, in atrial natriuretic peptide receptor-deficient mice [44], cardiac remodelling was also associated with enhanced NHE1 activity and stimulation of several molecular pathways, including CaMKII and Akt, the activity of these two pathways being regressed during reversal of the hypertrophic phenotype by NHE1 inhibitor treatment. In the present study, both CaMKII and Akt phosphorylation were stimulated by intracellular acidification in GK LV myocytes but, in contrast with the above-mentioned study, only Akt activity was markedly decreased by cariporide treatment. In this context, upregulation of Akt activity appears to play a major role in facilitating cell growth, and it has been shown, for example, that overexpression of H11 kinase in vitro in isolated cardiac myocytes, which promotes cardiac cell hypertrophy, essentially results in the activation of the Akt pathway, whereas the MAP kinase pathway is unaffected [35].

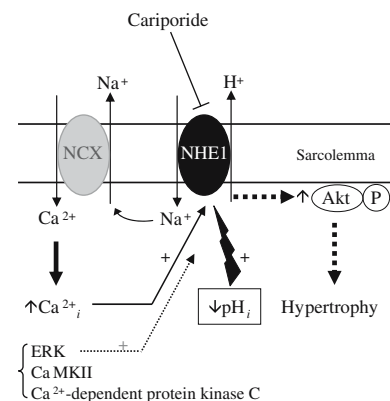


**Fig. 7** Proposed scheme for NHE1-dependent mechanisms of hypertrophy in GK LV myocytes. NHE1 activation is extremely sensitive to low  $pH_i$ , such as that which occurs during mild ischaemia. The resulting increases in  $\text{Na}_i^+$  generates  $\text{Ca}_i^{2+}$  increase via reverse  $\text{Na}^+-\text{Ca}^{2+}$  exchange (NCX).  $\text{Ca}_i^{2+}$  increase in turn contributes to maintaining elevated NHE1 activity. Elevated NHE1 activity leads to increased phosphorylation of Akt and, ultimately, to myocyte hypertrophy. Besides NHE1, increased  $\text{Ca}_i^{2+}$ , increased pAkt and hypertrophy were all reduced by cariporide treatment. Dotted arrows indicate intermediate steps

The question of whether the GK rats progress into manifest type 2 diabetes in older animals has not been addressed here. One recent work has shown that blood glucose continuously rose with age together with an impaired glucose tolerance in untreated GK rats [45]. Increased NHE1 activity in GK LV myocytes might have been expected to result in increased basal  $pH_i$ , which was not observed in the present study. However, steady-state  $pH_i$  in cardiac cells is the result of a balance between the activity of several membrane ionic carriers. The activation of NHE1 and of  $Na^+ - HCO_3^-$  co-transport induces an alkalinisation, whereas activation of the  $Cl^- - HCO_3^-$  exchanger triggers an acidification [46]. In a group of experiments that we performed with LV myocytes superfused with  $HCO_3^-$ -buffered solution (data not shown) we did not identify any change in the activity of the  $Na^+ - HCO_3^-$  cotransporter. However, results were suggestive of increased  $Cl^- - HCO_3^-$  exchanger activity that may well be sufficient to balance increased NHE1 activity at resting  $pH_i$ . The results here show that acidic  $pH_i$  values over the 6.8–6.9 range clearly revealed increased activity of NHE1, in agreement with the known activation characteristics of this carrier by internal  $H^+$  ions [13, 38]. The most likely explanation for such  $pH_i$  values in vivo is defective coronary blood flow, which has been observed in GK rat hearts [7, 47], and consequent mild ischaemia. We may also infer that this increase in NHE1 activity may have particularly deleterious functional consequences in cases of more severe ischaemia due to the consequent deleterious increase in  $Na_i^+$  [48].

**Conclusion** Our data illustrate a new mechanism by which the cardiac response to acidification, i.e. increased NHE1 activity and associated Akt activation, is coupled to the development of LV myocyte hypertrophy in the GK model of type 2 diabetes (Fig. 7). Although these data should be interpreted with caution inherent to the limitations of an animal model, they may contribute to shedding light on the central role that NHE1 may play in favouring LV hypertrophy in type 2 diabetic patients with impaired myocardial perfusion [49, 50] and therefore myocardial ischaemia in some circumstances.

**Acknowledgements** This work was supported by a grant from the Foundation of France. A. Darmellah and S. Tamareille were supported by fellowships from the French Ministry for Education and Research, and D. Baetz by a grant from the Medical Research Foundation. We wish to thank S. Bolte for expert support with confocal microscopy. The Imaging and Cell Biology facility of the Federative Research Institute 87 is supported by Support Services for Technology and Research of the General Council of Essonne. We also wish to thank C. Martens for critical reading of the manuscript.

**Duality of interest** The authors state that there is no duality of interest.

## References

1. Shehadeh A, Regan TJ (1995) Cardiac consequences of diabetes mellitus. *Clin Cardiol* 18:301–305
2. Devereux RB, Roman MJ, Paranicas M et al (2000) Impact of diabetes on cardiac structure and function: the strong heart study. *Circulation* 101:2271–2276
3. Struthers A, Morris A (2002) Screening for and treating left-ventricular abnormalities in diabetes mellitus: a new way of reducing cardiac deaths. *Lancet* 359:1430–1432
4. Frustaci A, Kajstura J, Chimenti C et al (2000) Myocardial cell death in human diabetes. *Circ Res* 87:1123–1132
5. Pierce GN, Maddaford TG, Russell JC (1997) Cardiovascular dysfunction in insulin-dependent and non-insulin-dependent animal models of diabetes mellitus. *Can J Physiol Pharmacol* 75:343–350
6. Belke DD, Swanson EA, Dillmann WH (2004) Decreased sarcoplasmic reticulum activity and contractility in diabetic *db/db* mouse heart. *Diabetes* 53:3201–3208
7. Desrois M, Sidell RJ, Gauguier D, Davey CL, Radda GK, Clarke K (2004) Gender differences in hypertrophy, insulin resistance and ischemic injury in the aging type 2 diabetic rat heart. *J Mol Cell Cardiol* 37:547–555
8. Portha B, Serradas P, Bailbe D, Suzuki K, Goto Y, Giroix MH (1991) Beta-cell insensitivity to glucose in the GK rat, a spontaneous nonobese model for type II diabetes. *Diabetes* 40:486–491
9. Gauguier D, Froguel P, Parent V et al (1996) Chromosomal mapping of genetic loci associated with non-insulin dependent diabetes in the GK rat. *Nat Genet* 12:38–43
10. Karmazyn M, Gan XT, Humphreys RA, Yoshida H, Kusumoto K (1999) The myocardial  $Na^+-H^+$  exchange: structure, regulation, and its role in heart disease. *Circ Res* 85:777–786
11. Khandoudi N, Bernard M, Cozzone P, Feuvray D (1990) Intracellular pH and role of  $Na^+/H^+$  exchange during ischaemia and reperfusion of normal and diabetic rat hearts. *Cardiovasc Res* 24:873–878
12. Khandoudi N, Bernard M, Cozzone P, Feuvray D (1995) Mechanisms of intracellular pH regulation during postischemic reperfusion of diabetic rat hearts. *Diabetes* 44:196–202
13. Le Prigent K, Lagadic-Gossmann D, Feuvray D (1997) Modulation by  $pH_o$  and intracellular  $Ca^{2+}$  of  $Na^+-H^+$  exchange in diabetic rat isolated ventricular myocytes. *Circ Res* 80:253–260
14. Stromer H, de Groot MC, Horn M et al (2000)  $Na^+/H^+$  exchange inhibition with HOE642 improves postischemic recovery due to attenuation of  $Ca^{2+}$  overload and prolonged acidosis on reperfusion. *Circulation* 101:2749–2755
15. Takewaki S, Kuro-o M, Hiroi Y et al (1995) Activation of  $Na^+-H^+$  antiporter (NHE-1), gene expression during growth, hypertrophy and proliferation of the rabbit cardiovascular system. *J Mol Cell Cardiol* 27:729–742
16. Kusumoto K, Haist JV, Karmazyn M (2001)  $Na^+/H^+$  exchange inhibition reduces hypertrophy and heart failure after myocardial infarction in rats. *Am J Physiol* 280:H738–H745
17. Engelhardt S, Hein L, Keller U, Klämbt K, Lohse MJ (2002) Inhibition of  $Na^+-H^+$  exchange prevents hypertrophy, fibrosis and heart failure in  $\beta_1$ -adrenergic receptor transgenic mice. *Circ Res* 90:814–819
18. Linz WJ, Busch AE (2003) NHE-1 inhibition: from protection during acute ischaemia/reperfusion to prevention/reversal of myocardial remodelling. *Naunyn Schmiedebergs Arch Pharmacol* 368:239–246
19. Chen Y, Escoubet B, Prunier F et al (2004) Constitutive cardiac overexpression of sarcoplasmic/endoplasmic reticulum  $Ca^{2+}$ -ATPase delays myocardial failure after myocardial infarction in rats at a cost of increased acute arrhythmias. *Circulation* 109:1898–1903

20. Rucker-Martin C, Pecker F, Godreau D, Hatem SN (2002) Dedifferentiation of atrial myocytes during atrial fibrillation: role of fibroblast proliferation in vitro. *Cardiovasc Res* 55:38–52
21. Baetz D, Haworth RS, Avkiran M, Feuvray D (2002) The ERK pathway regulates  $\text{Na}^+\text{-HCO}_3^-$  cotransport activity in adult rat cardiomyocytes. *Am J Physiol* 283:H2102–H2109
22. Satoh H, Delbridge LM, Blatter LA, Bers DM (1996) Surface: volume relationship in cardiac myocytes studied with confocal microscopy and membrane capacitance measurements: species-dependence and developmental effects. *Biophys J* 70:1494–1504
23. Chattou S, Coulombe A, Diacono J, Le Grand B, John G, Feuvray D (2000) Slowly inactivating component of sodium current in ventricular myocytes is decreased by diabetes and partially inhibited by known  $\text{Na}^+\text{-H}^+$  exchange blockers. *J Mol Cell Cardiol* 32:1181–1192
24. Lagadic-Gossmann D, Buckler KJ, Le Prigent K, Feuvray D (1996) Altered  $\text{Ca}^{2+}$  handling in ventricular myocytes isolated from diabetic rats. *Am J Physiol* 270:H1529–H1537
25. Wang J, Schwinger RH, Frank K et al (1996) Regional expression of sodium pump subunits isoforms and  $\text{Na}^+\text{-Ca}^{++}$  exchanger in the human heart. *J Clin Invest* 98:1650–1658
26. Wold LE, Dutta K, Mason MM et al (2005) Impaired SERCA function contributes to cardiomyocyte dysfunction in insulin-resistant rats. *J Mol Cell Cardiol* 39:297–307
27. Vasanji Z, Cantor EJ, Juric D, Moyen M, Netticadan T (2006) Alterations in cardiac contractile performance and sarcoplasmic reticulum function in sucrose-fed rats is associated with insulin resistance. *Am J Physiol Cell Physiol* 291:C772–C780
28. Richard P, Isnard R, Carrier L et al (1999) Double heterozygosity for mutations in the  $\beta$ -myosin heavy chain and in the cardiac myosin binding protein C genes in a family with hypertrophic cardiomyopathy. *J Med Genet* 36:542–545
29. Perez NG, de Hurtado MC, Cingolani HE (2001) Reverse mode of the  $\text{Na}^+\text{-Ca}^{2+}$  exchange after myocardial stretch: underlying mechanism of the slow force response. *Circ Res* 88:376–382
30. Tani M, Neely JR (1989) Role of intracellular  $\text{Na}^+$  in  $\text{Ca}^{2+}$  overload and depressed recovery of ventricular function of reperfused ischemic rat hearts. Possible involvement of  $\text{H}^+\text{-Na}^+$  and  $\text{Na}^+\text{-Ca}^{2+}$  exchange. *Circ Res* 65:1045–1056
31. Maly K, Strese K, Kampfer S et al (2002) Critical role of protein kinase C  $\alpha$  and calcium in growth factor induced activation of the  $\text{Na}^+\text{/H}^+$  exchanger NHE1. *FEBS Lett* 521:205–210
32. Schreckenber R, Taimor G, Piper HM, Schlüter K-D (2004) Inhibition of  $\text{Ca}^{2+}$ -dependent PKC isoforms unmasks ERK-dependent hypertrophic growth evoked by phenylephrine in adult ventricular cardiomyocytes. *Cardiovasc Res* 63:553–560
33. Snabaitis AK, Yokoyama H, Avkiran M (2000) Roles of mitogen-activated protein kinases and protein kinase C in  $\alpha_{1A}$ -adrenoceptor-mediated stimulation of the sarcolemmal  $\text{Na}^+\text{-H}^+$  exchanger. *Circ Res* 86:214–220
34. Moor AN, Fliegel L (1999) Protein-kinase-mediated regulation of the  $\text{Na}^+\text{/H}^+$  exchanger in the rat myocardium by mitogen-activated protein kinase-dependent pathways. *J Biol Chem* 274:22985–22992
35. Depré C, Hase M, Gaussin V et al (2002) H11 kinase is a novel mediator of myocardial hypertrophy in vivo. *Circ Res* 91:1007–1014
36. Wu KL, Khan S, Lakhe-Reddy S et al (2004) The NHE1  $\text{Na}^+\text{/H}^+$  exchanger recruits ezrin/radixin/moesin proteins to regulate Akt-dependent cell survival. *J Biol Chem* 279:26280–26286
37. Yang L, Dan HC, Sun M et al (2004) Akt/protein kinase B signaling inhibitor-2, a selective small molecule inhibitor of Akt signaling with antitumor activity in cancer cells overexpressing Akt. *Cancer Res* 64:4394–4399
38. Counillon L, Pouyssegur J (2000) The expanding family of eukaryotic  $\text{Na}^+\text{/H}^+$  exchangers. *J Biol Chem* 275:1–4
39. Hudmon A, Schulman H (2002) Structure-function of the multifunctional  $\text{Ca}^{2+}$ /calmodulin-dependent protein kinase II. *Biochem J* 364:593–611
40. Illario M, Cavallo AL, Bayer U et al (2003) Calcium/calmodulin-dependent protein kinase II binds to raf-1 and modulates integrin-stimulated ERK activation. *J Biol Chem* 278:45101–45108
41. Mukhin YV, Garnovskaya MN, Ullian ME, Raymond JR (2004) ERK is regulated by sodium-proton exchanger in rat aortic vascular smooth muscle cells. *J Biol Chem* 279:1845–1852
42. Jandeleit-Dahm K, Hannan KM, Farrelly CA et al (2000) Diabetes-induced vascular hypertrophy is accompanied by activation of  $\text{Na}^+\text{-H}^+$  exchange and prevented by  $\text{Na}^+\text{-H}^+$  exchange inhibition. *Circ Res* 87:1133–1140
43. Camilion de Hurtado MC, Portiansky EL, Perez NG, Rebollo OR, Cingolani HE (2002) Regression of cardiomyocyte hypertrophy in SHR following chronic inhibition of the  $\text{Na}^+\text{/H}^+$  exchanger. *Cardiovasc Res* 53:862–868
44. Kilic A, Velic A, De Windt LJ et al (2005) Enhanced activity of the myocardial  $\text{Na}^+\text{/H}^+$  exchanger NHE-1 contributes to cardiac remodeling in atrial natriuretic peptide receptor-deficient mice. *Circulation* 112:2307–2317
45. Rösen P, Wiernsperger NF (2006) Metformin delays the manifestation of diabetes and vascular dysfunction in Goto-Kakizaki rats by reduction of mitochondrial oxidative stress. *Diabetes Metab Res Rev* 22:323–330
46. Feuvray D (1997) The regulation of intracellular pH in the diabetic myocardium. *Cardiovasc Res* 34:48–54
47. Iltis I, Kober F, Desrois M et al (2005) Defective myocardial blood flow and altered function of the left ventricle in type 2 diabetic rats. *Invest Radiol* 40:19–26
48. Anzawa R, Bernard M, Tamarelle S et al (2006) Intracellular sodium increase and susceptibility to ischaemia in hearts from type 2 diabetic *db/db* mice. *Diabetologia* 49:598–606
49. Nahser PJ, Brown RE, Okarsson H, Winniford MD, Rossen JD (1995) Maximal coronary flow reserve and metabolic coronary vasodilation in patients with diabetes mellitus. *Circulation* 91:635–640
50. Nitenberg A, Ledoux S, Valensi P, Sachs R, Attali J-R, Antony I (2001) Impairment of coronary microvascular dilation in response to cold pressor-induced sympathetic stimulation in type 2 diabetic patients with abnormal stress thallium imaging. *Diabetes* 50:1181–1185